Published in final edited form as:
Biomacromolecules. 2010 April 12; 11(4): 919–926. doi:10.1021/bm9013364.

Polymeric Micelles with Ionic Cores Containing Biodegradable Crosslinks for Delivery of Chemotherapeutic Agents

Jong Oh Kim[1], **Gaurav Sahay**[1], **Alexander V. Kabanov**[1,2], and **Tatiana K. Bronich**[1,*]

[1]Department of Pharmaceutical Sciences and Center for Drug Delivery and Nanomedicine, College of Pharmacy, University of Nebraska Medical Center, 985830 Nebraska Medical Center, Omaha, NE 68198-5830

[2]Department of Chemistry, M.V. Lomonosov Moscow State University, Leninskie Gory, V-234, Moscow, 119992, Russia.

Abstract

Novel functional polymeric nanocarriers with ionic cores containing biodegradable cross-links were developed for delivery of chemotherapeutic agents. Block ionomer complexes (BIC) of poly (ethylene oxide)-*b*-poly(methacylic acid) (PEO-*b*-PMA) and divalent metal cations (Ca^{2+}) were utilized as templates. Disulfide bonds were introduced into the ionic cores by using cystamine as a biodegradable cross-linker. The resulting cross-linked micelles with disulfide bonds represented soft, hydrogel-like nanospheres and demonstrated a time-dependent degradation in the conditions mimicking the intracellular reducing environment. The ionic character of the cores allowed to achieve a very high level of doxorubicin (DOX) loading (50% w/w) into the cross-linked micelles. DOX-loaded degradable cross-linked micelles exhibited more potent cytotoxicity against human A2780 ovarian carcinoma cells as compared to micellar formulations without disulfide linkages. These novel biodegradable cross-linked micelles are expected to be attractive candidates for delivery of anticancer drugs.

Keywords

Block copolymeric micelles; disulfide bonds; doxorubicin; self-assembly; core-shell morphology

1. Introduction

Nanosized self-assembled polymeric micelles based on amphiphilic block copolymers have been extensively studied as potential delivery vehicles for anti-cancer drugs.[1-7] Such polymeric micelles can circumvent renal excretion and have increased circulation time in the body compared to the free drug. This can lead to increased accumulation of the micelle-incorporated drug in the tumors due to the enhanced permeability and retention (EPR) effect.[8] However, disintegration of multimolecular micelles after their dilution in biological milieu is a major drawback for their application *in vivo* since it can result in premature drug release. This problem can be addressed by introducing cross-links between the polymer chains, which can stabilize the micelles against dilution, ionic strength, temperature, and shear forces.[9-11] We recently described novel polymeric micelles with stably cross-linked ionic cores (*cl*-micelles) synthesized using template-assisted procedure.[9, 10] Such *cl*-micelles are made of

* Corresponding author: Tel: (402) 559-9351 Fax: (402) 559-9365 tbronich@unmc.edu .

Supporting Information Available: ^{1}H NMR and IR spectra, AFM and TEM images, DLS data on degradation of *cl*-micelles/Cys in the presence of DTT, and cytotoxicity curves. This material is available free of charge via the Internet at http://pubs.acs.org.

poly(ethylene oxide)-*b*-poly(methacrylic acid) (PEO-*b*-PMA) diblock copolymers and have cores of cross-linked PMA network surrounded by a shell of PEO chains. They can swell in aqueous environments and display pH- and ionic strength-responsive hydrogel-like behavior characteristic of ionic nanogels.[12] Various anti-cancer drugs such as doxorubicin (DOX) or cisplatin were successfully encapsulated into the *cl*-micelle ionic cores with high loading efficiency.[10, 13] The drug-loaded *cl*-micelles were shown to accelerate release of the drug in pH-dependent fashion in acidic environment due to the protonation of carboxylic groups in the cores of the micelles. It was further demonstrated that these materials can exploit differential endocytic pathways in cancer and normal epithelial cells to selectively deliver and release the drug in the cancer cells.[14] Since the molecular weight of *cl*-micelles is far above the renal threshold (~ 40 KDa for copolymers) after intravenous administration they cannot be removed from the body through renal excretion,[15] which can result in their long-term circulation. Furthermore, such materials are expected to have decreased extravasation into normal organs and increased accumulation in tumors through the EPR effect. However, since the *cl*-micelles are not degradable there is a concern of their long term accumulation in the body. This work describes a new type of *cl*-micelles with reversible cross-links containing disulfide bonds. Such cross-links are stable in extracellular milieu but are cleaved in the reducing environment of the cytoplasm of the cells due to the differences in the reductive potential between the extracellular and intracellular compartments. This approach has been previously successfully utilized in design of various polymeric carriers for anticancer drugs,[16, 17] imaging agents,[18, 19] plasmid DNA and antisense oligonucleotides.[20-23] We posit that *cl*-micelles with reversible cross-links will be stable in the bloodstream but labile once internalized in tumor cells thus facilitating the release of the drug. Furthermore, the induced cleavage of the cross-links will also result in degradation of the *cl*-micelles and release the individual copolymer chains, which can eventually be removed from the body by the renal clearance once the drug is delivered.

This paper describes synthesis of *cl*-micelles with cystamine as a biodegradable cross-linker. These micelles are evaluated *in vitro* for the controlled delivery of anti-cancer agent, DOX. First, the physicochemical properties and degradation of *cl*-micelles with disulfide bonds in the presence of reducing agents were characterized. Second, the loading of DOX in the *cl*-micelles and release of DOX from the *cl*-micelles in the presence of reducing agents were examined. Third, delivery of the drug-loaded *cl*-micelles in tumor cells is characterized by confocal microscopy. Finally, the drug-loaded *cl*-micelles with reduction-sensitive cross-links are compared with similar *cl*-micelles with non-degradable cross-links in *in vitro* cytotoxicity assay in tumor cells. Altogether, we demonstrate that degradable *cl*-micelles can facilitate the release and potentiate *in vitro* cytotoxicity of DOX compared to non-degradable micelles.

2. Experimental Section

2.1. Materials

PEO-*b*-PMA diblock copolymer (M_n 23,000, M_w/M_n = 1.45) was purchased from Polymer Source Inc., Canada. The repeating units for PEO and PMA blocks were 170 and 180, respectively. The concentration of carboxylate groups in the copolymer samples was determined by potentiometric titration. Calcium chloride, cystamine dihydrochloride (Cys), ethylenediamine (ED), 1-(3-dimethylaminopropyl)-3-ethylcarbodiimide hydrochloride (EDC), N-hydroxysuccinimide (NHS), triethylamine (TEA), methanol, dimethylformamide (DMF) and ethylenediaminetetraacetic acid (EDTA) were obtained from Sigma-Aldrich (St Louis, MO). Doxorubicin hydrochloride was a kind gift from Dong-A Pharmaceutical Company, South Korea. Lysotracker™ (red or green), fetal bovine serum (FBS) (both dialyzed and heat inactivated), DMEM and RPMI 1640 media were purchased from Invitrogen Inc (Carlsbad, CA). Bovine serum albumin (BSA) and NUNC™ chambered glass coverslips for live cell imaging were purchased from Fisher Scientific (Waltham, MA). MTT reagent (3-(4,5-

Dimethylthiazol-2-yl)-2,5-diphenyltetrazolium bromide) was purchased from Research Products International (Prospect, IL). All other chemicals were of reagent grade and used without further purification.

2.2. Synthesis of FITC-labeled PEO-b-PMA

To synthesize FITC-labeled PEO-*b*-PMA fluoresceninthiocarbamyl ethylenediamine (FITC-ED) was synthesized using previously reported procedure.[24] Briefly, ED (200 mg, 1.5 mM) was dissolved in mixture of 50 ml methanol and 0.5 ml TEA. Solution of FITC (117 mg, 0.3 mmol) in 10 ml methanol containing 100 μl TEA was added dropwise to ED solution over a 30 min period followed by stirring for additional 1 hr. The resulting solution was filtered and ED-FITC was recovered by precipitation in 10 ml of methanol. The precipitate was dried in air, and used without further purification. Then, PEO-*b*-PMA 100 mg (0.78 mmol carboxylic groups) was dissolved in 2.5 ml DMF. NHS (2 mg, 0.0174 mmol) and EDC (4.8 mg, 0.025 mmol) in dichloromethane (1.0 ml) were added to a solution of PEO-*b*-PMA. The reaction mixture was stirred overnight at room temperature (R.T.). After that, 4 mg of FITC-ED in 200 μl DMF and 20 μl TEA were added to the mixture and stirred for additional 12 hr. Organic solvents were evaporated in vacuum, and the mixture was dialyzed against distilled water for 2 days using a dialysis membrane (MW cutoff 3,500 Da). FITC-labeled PEO-*b*-PMA was further purified by size exclusion chromatography and lyophilized.

2.3. Synthesis of DOX-labeled PEO-b-PMA

NHS (2.34 mg, 0.02 mmol) and EDC (6.0 mg, 0.03 mmol) in dichloromethane (1.0 ml) were added to a solution of 100 mg PEO-*b*-PMA in 20 ml DMF/methanol (1:1 v/v) and stirred for 2 hr at R.T. DOX (9.1 mg, 0.016 mmol) and TEA (4.5 μl, 0.032 mmol) in methanol were added to this solution and the reaction mixture was stirred continuously for additional 24 hr. Organic solvents were evaporated in vacuum, and resulting mixture was dialyzed against distilled water for 2 days using a dialysis membrane (MW cutoff 3,500 Da). DOX-labeled PEO-*b*-PMA was further purified using size exclusion chromatography and lyophilized. The degree of conjugation was 2.7 DOX molecules per copolymer chain as determined by ^{1}H-NMR spectroscopy.

2.4. Synthesis of cl-micelles

The ***cl***-micelles were prepared using block ionomer complexes of PEO-*b*-PMA copolymer and divalent metal cations as templates by the previously described method.[9] Briefly, PEO-*b*-PMA/Ca^{2+} complexes or FITC- or DOX-labeled PEO-*b*-PMA/Ca^{2+} complexes were prepared by mixing an aqueous solution of corresponding PEO-*b*-PMA with a solution of $CaCl_2$ at a molar ratio of $[Ca^{2+}]/[COO^{-}]=1.3$ ($[COO^{-}]= 3.5$ mM, pH 7.8). The EDC was then added to the dispersion of PEO-*b*-PMA/Ca^{2+} complexes to create an active-ester intermediate with carboxylic groups of PMA. To prepare the *cl*-micelles with disulfide bonds (*cl*-micelles/Cys) this dispersion of activated PEO-*b*-PMA/Ca^{2+} complexes was supplemented with the solution of cystamine, a biodegradable disulfide-containing cross-linker. The degree of cross-linking was controlled by the ratio of amine functional groups of the cross-linker to carboxylic acid groups, which was varied from 10% to 70%. The reaction mixture was allowed to stir overnight at R.T. After completion of the reaction, EDTA (1.5 molar equivalent) was added followed by dialysis, first, against 0.5% aqueous ammonia, and, second, against distilled water to remove metal ions and byproducts of the cross-linking reaction. Similar procedure was used to prepare *cl*-micelles with non-biodegradable ionic cores using ED as a cross-linker (*cl*-micelles/ED).

2.5. Preparation of DOX-loaded cl-micelles

DOX-loaded *cl*-micelles were prepared by the previously described method.[13] Briefly, an aqueous dispersion of *cl*-micelles was mixed with an aqueous solution of DOX (2 mg/ml) at

a feeding ratio of R=0.5 (R is a molar ratio of DOX to carboxylate groups of the micelles) at pH 7.0, followed by incubation for 24 h at R.T. Unbound DOX was removed by ultrafiltration using Amicon YM-30 centrifugal filter devices pretreated with DOX (MWCO 30,000 Da, Millipore). Concentration of DOX in filtrates and in the micelles was determined by measuring the absorbance at 485 nm using Lambda 25 UV/VIS spectrophotometer.

2.6. Release studies of DOX-loaded cl-micelles

Release of DOX from the *cl*-micelles/Cys was studied by dialysis method using a membrane (MW cut-off 3,500 Da). 1 mL of DOX-loaded *cl*-micelles/Cys dispersions with DOX concentration of 0.2 mg/mL in phosphate buffered saline (PBS, pH 7.4, 0.14 M NaCl) were placed into a dialysis bags and dialyzed against 25 mL of PBS under continuous shaking at 37°C in dark. Reducing agents, glutathione (GSH) or cysteine were added at various concentrations (10 μM, 0.1 mM, 1 mM, 10 mM) in PBS. At a definite time interval (every 1h up to 8 h, and then at 24 h, 48 h, and 72 h), 1 mL samples of the dialysate solution were withdrawn and replaced with an equal volume of fresh media. The concentration of DOX in the dialysate samples was determined spectrophotometrically by measuring absorbance at 485 nm. The amount of DOX released from the micelles was expressed as a percentage of the total DOX and plotted as a function of time. For DOX-loaded *cl*-micelles the release rates were calculated from the initial rapid release stage using Baker-Lonsdale model.[25]

2.7. Size and ζ-potential measurements

"ZetaPlus" analyzer (Brookhaven Instrument Co.) with a 30 mW solid-state laser operating at a wavelength of 635 nm was used to determine effective hydrodynamic diameters (D_{eff}) and ζ-potential of the particles at 25°C. Effective hydrodynamic diameters (D_{eff}) of the particles were measured by photon correlation spectroscopy (DLS) in a thermostatic cell at a scattering angle of 90° using the same instrument equipped with a Multi Angle Sizing Option (BI-MAS). ζ-potential of the particles was calculated from the electrophoretic mobility values using Smoluchowski equation. Software provided by the manufacturer which employs cumulants analysis and non-negatively constrained least-squares (NNLS) particle size distribution analysis routines was used to analyze the size of the particles, polydispersity indices and ζ-potential of *cl*-micelles. The mean values were calculated from the measurements performed at least in triplicate.

2.8. Atomic Force Microscopy (AFM)

The tapping mode AFM imaging was performed in air using a Multimode NanoScope IV system (Veeco, Santa Barbara, CA). For AFM samples preparation, 5 μl of an aqueous dispersion of *cl*-micelles (ca. 1.0 mg/ml) was deposited onto positively charged 1-(3-aminopropyl)silatrane mica surface (APS-mica) for 2 min, followed by surface drying under argon atmosphere. The imaging in air was performed with regular etched silicon probes (TESP) with a spring constant of 42 N/m. The images were processed and the widths and heights of the particles were measured using Femtoscan software (Advanced Technologies Center, Moscow, Russia).

2.9. Transmission Electron Microscopy (TEM)

For TEM studies a drop of the sample solution was allowed to settle on a Formvar coated copper grid for 1 min. Excess sample was wicked away with filter paper, and a drop of 1% uranyl acetate solution was allowed to contact the sample for 20 s. The samples were air dried and studied using a Hitachi H-7000 microscope. The number average particle diameter values and standard deviations were determined using at least 70 measurements randomly collected from five TEM images using Image Pro program (Media Cybernetics).

2.10. Confocal microscopy on live cell

Cellular uptake of *cl*-micelles/Cys was characterized by live cell confocal imaging using Carl Zeiss LSM 510 Meta confocal microscope (Peabody, MA). Human ovarian carcinoma A2780 cells (1×10^6) were plated in live cell chambers (Fischer Scientific, Waltham, MA) and after two days (37°C, 5% CO_2) were exposed to FITC- or DOX-labeled *cl*-micelles for 60 min, followed by incubation with Lysotracker Red® for 10 min. Finally, cells were washed and kept in complete media for confocal imaging.

2.11. Cell transfection

A2780 cells were transfected using Organelle Lights™ Endosome-GFP kit. This kit includes Organelle Lights™ reagent, which is baculovirus that contains a gene sequence encoding an early endosome marker Rab5a (targeting sequence) or Actin fused to a Green Fluorescent Protein (GFP) incorporated into the viral genome. The kit also includes an enhancer solution for increased expression of the chimera. Briefly, cells were plated, allowed to attach, and treated with Organelle Lights reagent at R.T. in the dark for 2-4 hrs. The reagent was aspirated and cells were incubated in RPMI-1640 medium containing 1X enhancer for 2 hrs followed by washing and addition of complete medium. The transfected cells were treated with DOX-labeled *cl*-micelles/Cys for 60 min, washed, and imaged using confocal microscopy. In select experiments A2780 cells were transfected with plasmid DNA (1μg/ml) encoding K44A dynamin mutant using Lipofectamine™ 2000 as previously described.[26]

2.12. In vitro cytotoxicity studies

Cytotoxicity of DOX-loaded *cl*-micelles was assessed in A2780 cells by a standard MTT assay as described previously.[10] Briefly, cells were seeded in a 96-well microtiter plates with 10,000 cells per well and allowed to adhere for 24 h prior to the assay. Cells were exposed to various doses (0–200 g/ml on DOX basis) of DOX alone, polymeric micelles alone, and DOX-loaded *cl*-micelles for 24 h at 37 °C, followed by washing with PBS, and maintaining in RPMI 1640 medium with 10% FBS for additional 72 h. The 25 l of MTT indicator dye (5 mg/ml) was added to each well and the cells were incubated for 2 h at 37°C in the dark. The 100 l of 50% DMF-20% SDS solution was added to each well and kept overnight at 37 °C. Absorption was measured at 570 nm in a microplate reader (SpectraMax M5, Molecular Devices Co., USA) using wells without cells as blanks. All measurements were taken eight times. Based on the results of the test, the IC_{50} values (the concentration which kill 50% of cells) were calculated by using GraphPad Prism Software (GraphPad Software, San Diego California, USA).

3. Results and Discussion

3.1. Synthesis of cl-micelles with disulfide bonds

The general scheme for the synthesis of *cl*-micelles is presented in Figure 1. Biodegradable disulfide bonds were introduced into the micellar cores using cystamine as a cross-linker. The *cl*-micelles/Cys with various targeted degrees of cross-linking from 10% to 70% were prepared using the same stock solution of template PEO-*b*-PMA/Ca^{2+} micelles. It is important to point out that the “targeted” degree of cross-linking represents the maximum theoretical amount of cross-links that can form rather than the actual number of cross-links, which was shown to be lower than the theoretical value.[9] Similar procedure was utilized to prepare the set of the *cl*-micelles/ED with non-degradable cross-links in the cores using ED as cross-linker. We have previously described such structures as hydrogel-like soft nanomaterials with cores comprised a network of the cross-linked polyanions surrounded by a flexible hydrophilic shell composed of PEO blocks. Figures 2A and 2B present the hydrodynamic diameters (D_{eff}) and ζ-potentials of *cl*-micelles/Cys and *cl*-micelles/ED with 20% targeted degree of cross-linking. Upon increase of pH, both types of *cl*-micelles underwent significant swelling due to ionization of

the PMA chains in the micelles core (Figure 2A), which was also accompanied by the considerable increase of net negative ζ-potential (Figure 2B). In addition, the swelling of *cl*-micelles was also strongly affected by the degree of cross-linking. The sizes of *cl*-micelles with various cross-linking densities are presented in Figure 2C. As expected, the increase of the targeted degree of cross-linking resulted in decrease of the size of the *cl*-micelles. The micelles with lower degrees of cross-linking had greater D_{eff}, while the micelles with higher degrees of cross-linking (40% or higher) exhibited only a modest increase in D_{eff} compared to the precursor block ionomer complex (Deff ≈ 90 nm). Interestingly, the overall swelling of *cl*-micelles/Cys was less pronounced compared to *cl*-micelles/ED at any given pH and targeted degree of cross-linking. Such behavior can be ascribed to a difference in actual number of cross-links formed during the synthesis of these micelles. We posit that since the core of the precursor PEO-*b*-PMA/Ca^{2+} micelles is relatively hydrophobic the reactive groups in this core are less accessible to a rather hydrophilic ED than to more hydrophobic Cys. As a result at the same targeted degree of cross-linking the actual number of cross-links in *cl*-micelles/Cys core may be higher compared to *cl*-micelles/ED. Due to the colloidal nature of the micelles, the conventional solution-state ^{1}H NMR does not permit to determine the precise number of cross-links per micelle. However, this technique allowed us to monitor, at least qualitatively, the changes in the extent of cross-linking upon the synthesis. Indeed, the integral intensity of the signal due to the methylene protons adjacent to amide groups (resonance at † ~3.2 – 3.3 ppm) progressively increased as the targeted degree of cross-linking increased from 20% to 60% (Figure S2). These measurements were done at pH 10 when the cores of the *cl*-micelles were completely swollen and the hindrance of the amide groups in the cores was expected to be minimal. At any given targeted degree of cross-linking an estimated number of amide bonds formed by the cross-linkers in the *cl*-micelles/Cys was ca. 1.8-fold higher than in *cl*-micelles/ED. For instance, at 20% targeted cross-linking assuming that all molecules of cross-linkers incorporated in *cl*-micelles formed two amide bonds with two different PMA chains the number of cross-links in *cl*-micelles/Cys was ca. 7 compared to only 4 in *cl*-micelles/ED. At 70% targeted cross-linking these numbers were 16 and 9 for *cl*-micelles/Cys and *cl*-micelles/ED, respectively. The IR spectroscopy also indirectly confirmed the difference in the extent of cross-linking between *cl*-micelles/Cys and *cl*-micelles/ED (Supporting Information, Figure S3). PEO-*b*-PMA copolymer shows a broad OH band centered in the range 2700-3300 cm^{-} which overlaps with C-H stretch, C=O stretching vibrations from the carbonyl groups at 1691 cm^{-}, and C-O stretch at 1242 cm^{-} and 1078 cm^{-}, respectively. For *cl*-micelle samples the carbonyl absorption bands were shifted to higher frequencies and amide II bands appeared at ca. 1575 cm^{-}, which confirms the formation of amide bonds in the micelles. The relative intensity of absorption band associated with amide bond was higher in *cl*-micelles/Cys than in *cl*-micelles/ED suggesting that at the same targeted degree of cross-linking the actual extent of modification in *cl*-micelles/Cys core is higher compared to *cl*-micelles/ED. An examination of size and shape of the *cl*-micelles in solid state by AFM and TEM provide further information regarding the microstructure of these nanoparticles. The typical images of *cl*-micelles/Cys and *cl*-micelles/ED with targeted degree of cross-linking of 20% are presented in Supporting Information (Figures S4 and S5). Both *cl*-micelles/Cys and *cl*-micelles/ED had a spherical morphology. As expected the number-average particle height (H_{av}) and diameter (D_{av}) values of dehydrated *cl*-micelles were reduced compared to the hydrodynamic diameters D_{eff} determined by DLS (Table 1). Upon adsorption on mica surface *cl*-micelles exhibited a high diameter versus height aspect ratios suggesting substantial flattering of the particles. This observation was in agreement with the expected flexible, shape-adaptable character of the *cl*-micelles imparted by the PMA “soft” core material. Interestingly, the *cl*-micelles/Cys were characterized by a significantly lower aspect ratio (ca. 12.2) compared to *cl*-micelles/ED (aspect ratio is 38.1). These data suggest that increased number of cross-links within the PMA core of *cl*-micelles/Cys provided substantial reinforcement of the cores of the micelles and resulted in the formation of relatively more stiff nanostructures. Therefore, the structure of

cross-linker (Cys vs. ED) appeared to directly affect the efficacy of cross-linking and the macroscopic characteristics and swelling behavior of the *cl*-micelles.

3.2 In vitro degradation of cl-micelles

Our next goal was to determine whether the disulfide bonds in the core of *cl*-micelles/Cys undergo cleavage in the presence of reducing agents. The degradability of *cl*-micelles/Cys was determined by incubating the micelles with DTT followed by analysis of the reaction mixture using size exclusion chromatography. Figure 3A shows elution profiles of *cl*-micelles/Cys (70% targeted degree of cross-linking) before and after incubation with DTT (25 mM) for various times at 37°C. As is seen, treatment with DTT resulted in gradual disappearance of the peak corresponding to *cl*-micelles over the incubation time and formation of products of significantly lower molecular masses. Specifically, an increase in the signal intensity at elution volume of ca. 12 ml corresponding to the initial PEO-*b*-PMA copolymers was observed over the same time period. Furthermore, decrease in light scattering intensity along with the drastic increase of polydispersity index was detected by dynamic light scattering of the *cl*-micelles/Cys dispersions already after 2 hr of incubation with DTT suggesting structural disintegration of such *cl*-micelles/Cys. The degradation rate of *cl*-micelles increased as the concentration of DTT increased (Figure S6A). In contrast, non-degradable *cl*-micelles/ED remained stable and no changes in their size were observed in the presence of DTT (Figure S6B). Changes in topology of *cl*-micelles/Cys as a result of their degradation were further characterized by utilizing tapping mode AFM. In the absence of DTT, *cl*-micelles/Cys appeared to be circular particles with the number averaged height of 4.3 ± 0.03 nm and diameter of 38.5 ± 0.2 nm (Figure 3B). The mixed population of tiny particles and fibrous materials was observed in AFM images of *cl*-micelles/Cys incubated with DTT (25 mM, 3 hr at 37 °C) (Figure 3C). Overall, these results imply that the synthesized *cl*-micelles/Cys with disulfide-containing cross-links in the cores were reduction-sensitive and rapidly degraded in the presence of the reducing agent.

3.3 DOX loading and release from cl-micelles

The ionic character of the core of the *cl*-micelles allows for the encapsulation of charged therapeutic molecules. In our previous study, we demonstrated that DOX can be efficiently encapsulated in the cores of *cl*-micelles/ED at pH 7.0, when both the DOX molecule and the carboxylic groups of the PMA cores were completely ionized and oppositely charged.[13] In the present study DOX was incorporated into *cl*-micelles/Cys using a similar procedure.[13] The physicochemical characteristics of DOX-loaded *cl*-micelles/Cys are presented in Table 1. The binding of DOX with the ionic core of *cl*-micelles/Cys was accompanied with a considerable decrease in the net negative ζ-potential (from ca. −27 mV to ca. −14 mV), similar to DOX-loaded *cl*-micelles/ED. However, in contrast to c*l*-micelles/ED,[13] the diameter of *cl*-micelles/Cys practically did not change upon loading with DOX. This may be due to less pronounced swelling of initial unloaded *cl*-micelles/Cys compared to c*l*-micelles/ED discussed above. Both types of DOX-loaded *cl*-micelles maintained their spherical morphology while exhibited significantly greater heights when adsorbed on the mica (Table 1). The dimension aspect ratio decreased significantly compared to the empty *cl*-micelles and suggests that the cores of the micelles became more rigid due to the DOX binding. It should be noted that incorporation of DOX into *cl*-micelles/Cys with relatively more rigid cores (higher extent of cross-linking) did not result in such pronounced changes in the dimensions compared to the initial *cl*-micelles as was observed for *cl*-micelles/ED: the dimension aspect ratio changed from 12.2 to 2.9 for *cl*-micelles/Cys and from 38.1 to 2.9 for *cl*-micelles/ED, respectively.

Notably, introduction of relatively hydrophobic Cys cross-linkers into the cores of *cl*-micelles/Cys did not affect their loading capacity compared to the *cl*-micelles/ED. Indeed, the loading capacity of DOX-loaded *cl*-micelles/Cys at pH 7.0 was ca. 51%, which was similar to the

capacity of *cl*-micelles/ED with the same degree of cross-linking of 20%. Furthermore, as expected both types of micelles with higher degree of cross-linking of 70% exhibited lower loading than the micelles with lower degree of cross linking (Table 1). This difference cannot be simply explained by the decrease in the total amount of carboxylate groups available for binding of DOX because in all cases the numbers of carboxylate groups consumed by the amide bonds appears to be less than 10%. However, there may be differences in the spatial distribution of the cross-links which may result in lower accessibility of the bulk of the carboxylate groups in the micelle cores. Alternatively, it is possible, NMR used to assess of the number of the amide groups significantly underestimates the amounts of these groups, due to colloidal nature of *cl*-micelles.

Of particular interest was the finding that the nature of the cross-linker in the micelle core affected the DOX release profiles. The release profiles of the DOX-loaded *cl*-micelles (20% targeted cross-linking) in PBS (pH 7.4, 0.14 M NaCl) are depicted in Figure 4A. For both types of the *cl*-micelles the release of DOX was characterized by two distinct stages with a relatively rapid release over the first 8 h followed by a slow release over 40 h. The data for the initial rapid release stage were fitted to rate equations based on diffusion considerations (Baker-Lonsdale model[25] of the release from the matrixes of the spherical shape) and the plots showed very good correlation coefficients of 0.990 and 0.994 for *cl*-micelles/Cys and *cl*-micelles/ED, respectively. Hence, the rate-determining step of DOX release from *cl*-micelles appeared to be controlled by diffusion. However, the release rates of DOX from *cl*-micelles/Cys were substantially less than those from *cl*-micelles/ED. For instance, at 8 h *cl*-micelles/Cys released only 38.6 ± 5.2 % of DOX, whereas *cl*-micelles/ED released 57.5 ± 9.7%. This phenomenon may be explained by differences in the swelling behavior of the *cl*-micelles described above assuming that the drug diffusion from the more swellable *cl*-micelles/ED is higher than from less swellable *cl*-micelles/Cys. We also cannot exclude that DOX molecules are better retained in the cores of *cl*-micelles/Cys due to hydrophobic interactions, although this possibility is less likely since we did not observe much difference in the loading between these two types of micelles.

To evaluate whether the degradation of *cl*-micelles/Cys in the reductive environment can trigger the drug release, DOX release from *cl*-micelles/Cys was further examined in PBS buffer in the presence of various concentrations cysteine or GSH, a tripeptide (L-γ-glutamyl-L-cysteinylglycine) that is the most abundant non-protein thiol-source in mammalian cells. As shown in Figure 4B and 4C, significant acceleration of DOX release from *cl*-micelles/Cys was observed in the presence of GSH or cysteine in the release media. The release rates were increased as the amount of reducing agent in the media increased. In particular, ca.75% of DOX was released from micelles within 1 h in the presence of 10mM GSH. In contrast, at low concentrations of GSH (10 μM) or cysteine (10 μM) mimicking the concentration of reducing agents in the bloodstream, the DOX release from *cl*-micelles/Cys was not considerably affected and was comparable with DOX release rates in the absence of reducing agents in the media. These results indicate that DOX release can be facilitated in the intracellular reducing environment by the cleavage of disulfide bonds in the cores of *cl*-micelles/Cys.

3.4 Intracellular delivery of cl-micelles and in vitro cytotoxicity

It is well accepted that the macromolecules and nanomaterials utilize multiple endocytic routes of internalization in the cells, which, in turn, affects their sorting to different compartments within the cell. The cleavage of disulfide bonds may proceed at various endocytic transport steps including cell surface and different endocytic organelles, as well as in cytosol. Therefore, to address the question where disulfide bonds in *cl*-micelles/Cys can be reduced, it was essential to understand how these polymer nanostructures enter and traffic in the cells. We evaluated the initial, intermediate and later stages of the itinerary of *cl*-micelles/Cys in human ovarian

adenocarcinoma A2780 cells. To examine initial stage, A2780 cells were transfected with a dynamin mutant K44A-GFP, which inhibits both caveolae- and clathrin-dependent endocytosis.[27, 28] It was found that the entry of DOX-labeled *cl*-micelles/Cys into A2780 cells expressing dynamin mutant was considerably decreased compared to non-transfected A2780 cells (Figure 5) suggesting that the micelles use a dynamin-dependent pathway. Interestingly, A2780 virtually do not express caveolin-1 as was previously reported[29] and confirmed in our studies (data not shown), which precludes formation of caveolae in these cells. In addition, little if any co-localization of *cl*-micelles/Cys with transferrin (Tf), marker of clathrin-mediated endocytosis, was observed in A2780 cell during first 20 min post incubation (Figure 6A and B). Altogether, these data suggest that initial stages of cellular trafficking of *cl*-micelles/Cys in A2780 cells most likely do not involve the caveolae- and clathrin-dependent pathways. An alternative mechanism of entry that can be exploited by these micelles in these cells is a dynamin/lipid raft dependent and clathrin-independent pathway.[30]

At the intermediate stage of entry (ca. 10 min) the *cl*-micelles/Cys were found to co-localize with Rab 5-GFP, a marker for early endosomes (Figure 7A). Finally, at the later stages (ca. 30 min) *cl*-micelles/Cys co-localized with a lysosomal marker, Lysotracker Red® (Figure 7B). Therefore, such micelles following the initial entry are routed first to early endosomes and then to late endosomes and/or lysosomes. Consistently with these finding, a co-localization of *cl*-micelles/Cys and Tf in A2780 cells was also observed at the later stages (30 min.) (Figure 6C). At this point Tf is known to reach recycling endosomes or lysosomal compartments.[31, 32] In lysosomes the reduction of disulfide bonds in the cores of *cl*-micelles/Cys can be enhanced by cysteine and presence of gamma-interferon inducible lysosomal thiol reductase.[33] It is also possible that the reductive degradation of *cl*-micelles/Cys may proceed at early stages of endocytic pathway. Indeed, it was demonstrated that the reduction of disulfide-linked folate conjugate in folate receptor-mediated endocytosis begins in the early endosomes.[34] In addition, redox machinery located at the cell surface can mediate the reduction of *cl*-micelles/Cys upon their interaction with the plasma membrane that engulfs these micelles.

Next, we evaluated whether the incorporation of DOX into *cl*-micelles/Cys can facilitate the cytotoxic activity of the drug in A2780 ovarian cancer cells. The cytotoxicity of DOX-loaded *cl*-micelles/Cys and DOX-loaded *cl*-micelles/ED was assessed using MTT assay. The IC_{50} values are summarized in Table 2. As expected, DOX-loaded *cl*-micelles displayed lower cytotoxic activity than free DOX. The reduction in cytotoxicity of DOX incorporated into *cl*-micelles was consistent with the sustained release of the drug. However, we found that degradable DOX-loaded *cl*-micelles/Cys were more cytotoxic compared to non-degradable DOX-loaded *cl*-micelles/ED. Indeed, IC_{50} value of DOX-loaded *cl*-micelles/Cys was at least six times less than that of *cl*-micelles/ED. This result was consistent with increased rates of DOX release from *cl*-micelles/Cys in the presence of reducing agent (Figure 4). Specifically, in the presence of 10 mM of glutathione the release rate was ca. 24.6 μg/h, 30.8-fold faster than in non-reductive environment and 12.6-fold faster than the drug release rate from *cl*-micelles/ED (ca. 1.96 μg/h). The release rate from DOX-loaded *cl*-micelles/Cys was also increased (ca. 3.7 μg/h, 1.9-fold faster that for DOX-loaded *cl*-micelles/ED) in the presence of cysteine, which is responsible for maintaining the proper level of redox potential in the endosomes/lysosomes. Importantly, both types of *cl*-micelles alone were not toxic at concentrations used for the treatment by DOX-loaded *cl*-micelles. Interestingly, DOX-loaded *cl*-micelles/Cys incubated with reducing agent for 24 h (DTT, 25 mM) before exposure to the cells displayed practically the same IC_{50} value (0.026 μM) that a free DOX at the same dose (0.024 μM) suggesting that DOX was completely recovered in active form from degraded *cl*-micelles/Cys (Figure S7). Therefore, the significant difference in the cytotoxic effect between DOX-loaded *cl*-micelles/Cys and DOX-loaded *cl*-micelles/ED suggest that intracellular degradation of the *cl*-micelles potentiated the release and cytotoxic activity of DOX.

4. Conclusion

We have developed a new type of cross-linked polymeric micelles with ionic cores containing reductively labile disulfide bonds. The DOX incorporation into and release from such biodegradable *cl*-micelles were investigated. Such micelles are characterized with very high drug loading (51% w/w). The type of cross-links (reduction-sensitive vs non-sensitive) substantially affected the release rates and cytotoxic activity of DOX. The strategy of reductive activation of micelle degradation can also facilitate the removal of the copolymer chains after drug release. Development of stimuli responsive nanomedicines that can deliver and release anticancer agents within the tumors can provide novel modality for efficient therapy of cancer and other human diseases. The polymeric micelles with cross-linked ionic cores responding to the intracellular environment appear to be a promising example of such clinically relevant carriers for delivery of anticancer drugs.

Supplementary Material

Refer to Web version on PubMed Central for supplementary material.

Acknowledgments

This work was supported by National Institutes of Health grant CA116590 to T.K.B. and UNMC Bukey Fellowship to G.S. The authors are grateful to Nanomaterials Core (supported by NIH COBRE Nebraska Center for Nanomedicine, grant 1P20RR021937) for assistance with characterization of *cl*-micelles, UNMC Nanoimaging Core (supported by grants from NIH SIG program, UNMC Program of Excellence and Nebraska Research Initiative) and Dr. Luda Shlyakhtenko for assistance with AFM studies. We would like to thank the NMR and Confocal Microscopy Core Facilities at UNMC for excellent technical assistance, Tom Bargar (Core Electron Microscopy Research Facility, UNMC) for acquisition of TEM images, Dr. Abijah Nyong for assistance with IR studies and Sunghee Chang for the help in the preparation of illustration for this paper.

References

(1). Rösler A, Vandermeulen GWM, Klok HA. Adv. Drug Delivery Rev 2001;53:95–108.

(2). Croy SR, Kwon GS. Curr. Pharm. Des 2006;12:4669–4684. [PubMed: 17168771]

(3). Riess G. Prog. Polym. Sci 2003;28:1107–1170.

(4). Allen C, Maysinger D, Eisenberg A. Colloids Surf., B 1999;16:3–27.

(5). Carlsen A, Lecommandoux S. Curr. Opin. Colloid Interface Sci 2009;14:329–339.

(6). Torchilin V. Eur. J. Pharm. Biopharm 2009;71:431–444. [PubMed: 18977297]

(7). Bronich TK, Nehls A, Eisenberg A, Kabanov VA, Kabanov AV. Colloids Surf., B 1999;16:243–251.

(8). Maeda H. Adv. Enzyme Regul 2001;41:189–207. [PubMed: 11384745]

(9). Bronich TK, Keifer PA, Shlyakhtenko LS, Kabanov AV. J. Am. Chem. Soc 2005;127:8236–8237. [PubMed: 15941228]

(10). Bontha S, Kabanov AV, Bronich TK. J. Controlled Release 2006;114:163–174.

(11). Bronich TK, Bontha S, Shlyakhtenko LS, Bromberg L, Hatton TA, Kabanov AV. J. Drug Target 2006;14:357–366. [PubMed: 17092836]

(12). Kabanov AV, Vinogradov SV. Angew. Chem., Int. Ed 2009;48:5418–5429.

(13). Kim JO, Kabanov AV, Bronich TK. J. Controlled Release 2009;138:197–204.

(14). Sahay G, Kim JO, Kabanov AV, Bronich TK. Biomaterials 2010;31:923–933. [PubMed: 19853293]

(15). Haag R, Kratz F. Angew. Chem., Int. Ed 2006;45:1198–1215.

(16). Oh JK, Siegwart DJ, Lee HI, Sherwood G, Peteanu L, Hollinger JO, Kataoka K, Matyjaszewski K. J. Am. Chem. Soc 2007;129:5939–5945. [PubMed: 17439215]

(17). Koo AN, Lee HJ, Kim SE, Chang JH, Park C, Kim C, Park JH, Lee SC. Chem. Commun 2008;48:6570–6572.

(18). Lu ZR, Wang X, Parker DL, Goodrich KC, Buswell HR. Bioconjugate Chem 2003;14:715–719.

(19). Ke T, Feng Y, Guo J, Parker DL, Lu ZR. Magn. Reson. Imaging 2006;24:931–940. [PubMed: 16916710]

(20). Neu M, Germershaus O, Mao S, Voigt KH, Behe M, Kissel T. J. Controlled Release 2007;118:370–380.

(21). Kakizawa Y, Harada A, Kataoka K. Biomacromolecules 2001;2:491–497. [PubMed: 11749211]

(22). Miyata K, Kakizawa Y, Nishiyama N, Harada A, Yamasaki Y, Koyama H, Kataoka K. J. Am. Chem. Soc 2004;126:2355–2361. [PubMed: 14982439]

(23). Miyata K, Kakizawa Y, Nishiyama N, Yamasaki Y, Watanabe T, Kohara M, Kataoka K. J. Controlled Release 2005;109:15–23.

(24). Pourfarzaneh M, White GW, Landon J, Smith DS. Clin. Chem 1980;26:730–733. [PubMed: 6768472]

(25). Radin S, Chen T, Ducheyne P. Biomaterials 2009;30:850–858. [PubMed: 19010531]

(26). Gebhart CL, Kabanov AV. J. Controlled Release 2001;73:401–416.

(27). Schlunck G, Damke H, Kiosses WB, Rusk N, Symons MH, Waterman-Storer CM, Schmid SL, Schwartz MA. Mol. Biol. Cell 2004;15:256–267. [PubMed: 14617821]

(28). Cobbold C, Coventry J, Ponnambalam S, Monaco AP. Hum. Mol. Genet 2003;12:1523–1533. [PubMed: 12812980]

(29). Hamelers IH, Staffhorst RW, Voortman J, de Kruijff B, Reedijk J, van Bergen en Henegouwen PM, de Kroon AI. Clin. Cancer Res 2009;15:1259–1268. [PubMed: 19228729]

(30). Doherty GJ, McMahon HT. Annu. Rev. Biochem 2009;78:857–902. [PubMed: 19317650]

(31). Gruenberg J, Maxfield FR. Curr. Opin. Cell Biol 1995;7:552–563. [PubMed: 7495576]

(32). Sahay G, Batrakova EV, Kabanov AV. Bioconjugate Chem 2008;19:2023–2029.

(33). Saito G, Swanson JA, Lee KD. Adv. Drug Delivery Rev 2003;55:199–215.

(34). Yang J, Chen H, Vlahov IR, Cheng JX, Low PS. Proc. Natl. Acad. Sci. U.S. A 2006;103:13872–13877. [PubMed: 16950881]

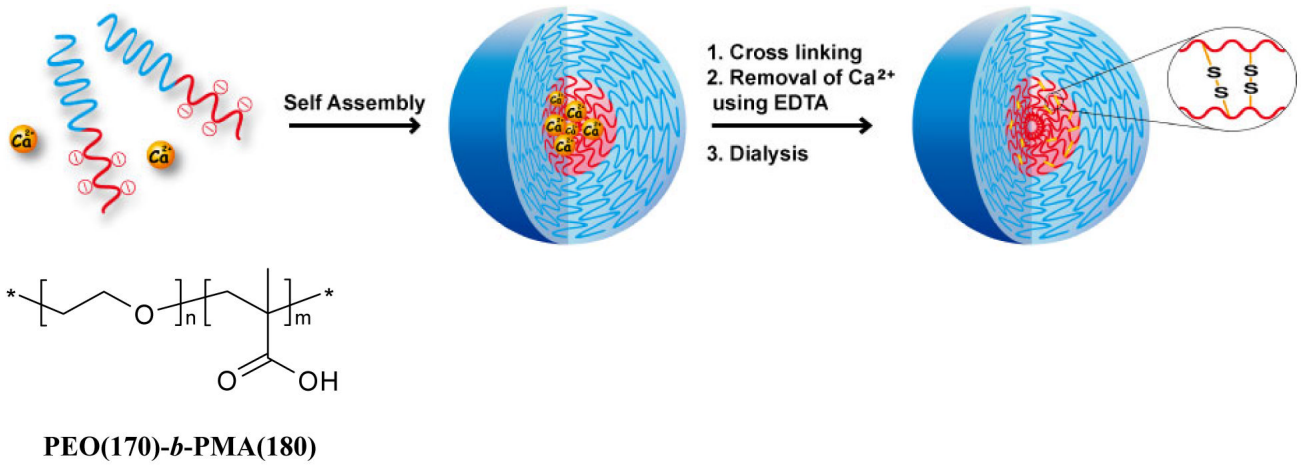

PEO(170)-*b*-PMA(180)

Figure 1.
Synthesis of PEO-*b*-PMA *cl*-micelles/Cys.

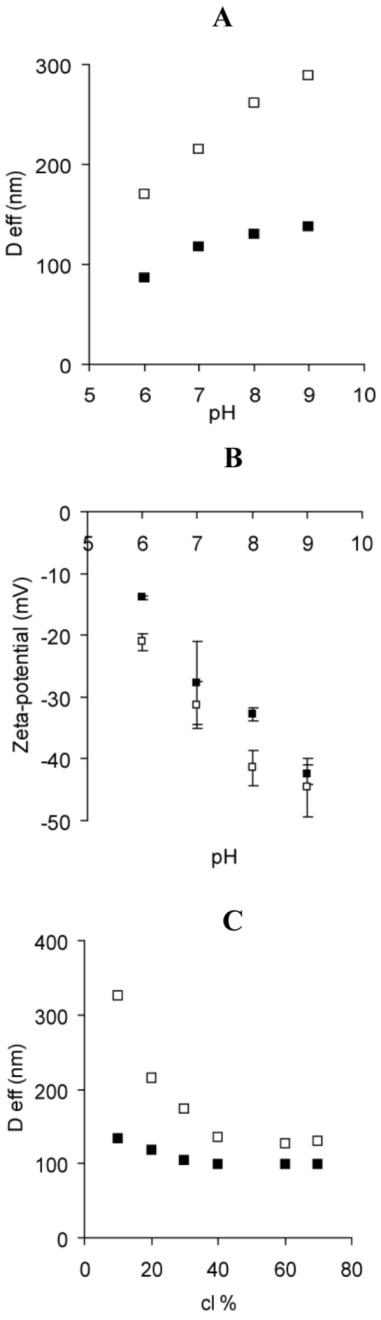

Figure 2.

Physicochemical characterization of *cl*-micelles with different cross-linkers: cystamine (■) and ethylenediamine (□). **(A)** Effective diameter (D_{eff}) and **(B)** ζ-potential with 20% targeted degree of cross-linking as a function of pH. **(C)** Effective diameter at pH 7.0. Data for *cl*-micelles/ED was modified from Ref [20].

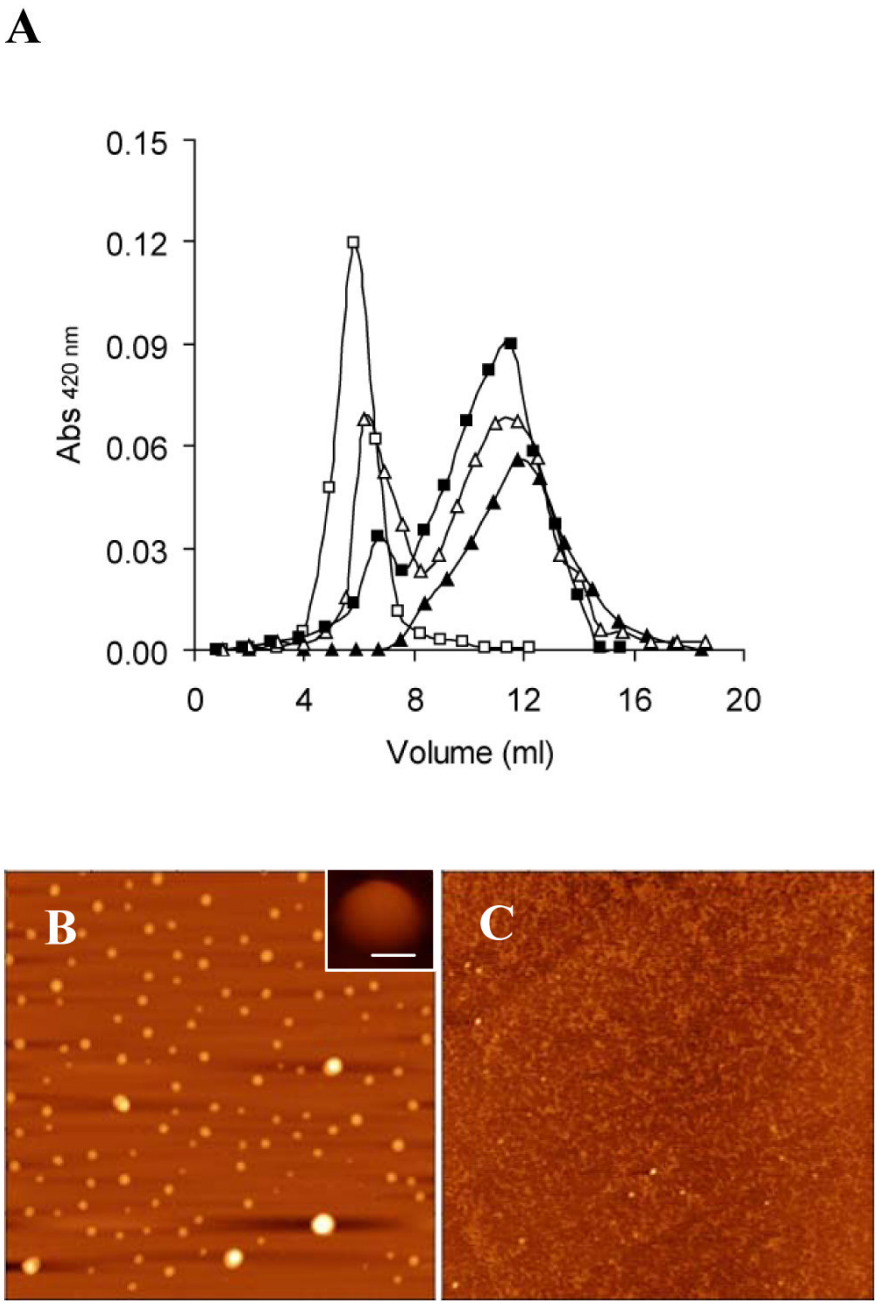

Figure 3.

In vitro biodegradability of *cl*-micelles/Cys with disulfide bonds. **(A)** Size-exclusion chromatograph. PEO-*b*-PMA copolymer (▲); *cl*-micelles/Cys without DTT (□); *cl*-micelles/Cys after incubation with DTT 25mM for 1 hour (Δ) and for 3hours (■). Tapping mode AFM images in air of *cl*-micelles/Cys after incubation without **(B)** and with DTT 25 mM for 3 hours **(C)** at 37 °C at pH 7.4. Targeted degree of cross-linking is 70%. Scan size of AFM images is 2 μm. The inserts show 3D image of the same micelles. Bar equals 20 nm.

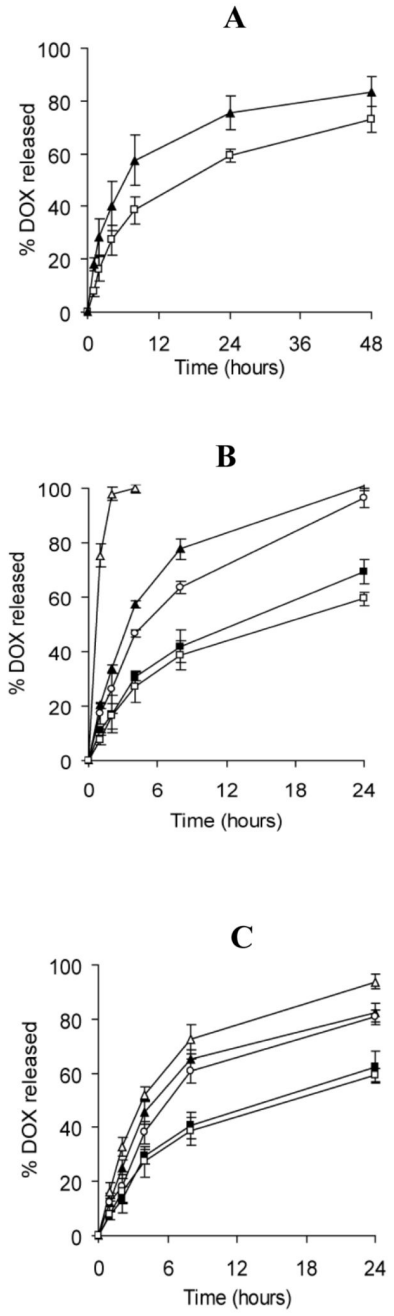

Figure 4.

(A) Release profiles of DOX from *cl*-micelles in PBS buffer (0.14 M NaCl, pH 7.4) at 37 °C. Degree of cross-linking is 20%. (□) *cl*-micelles/Cys and (▲) *cl*-micelles/ED. Release profiles of DOX from *cl*-micelles/Cys with in the presence of **(B)** glutathione and **(C)** cysteine in PBS buffer (0.14 M NaCl, pH 7.4). (□) control, (■) 10 μM, (○) 0.1 mM, (▲) 1 mM, (□) 10 mM. The loading amount of DOX for each sample is 200 μg. The data expressed average and standard deviation of three independent measurements. Data for *cl*-micelles/ED was modified from Ref [20].

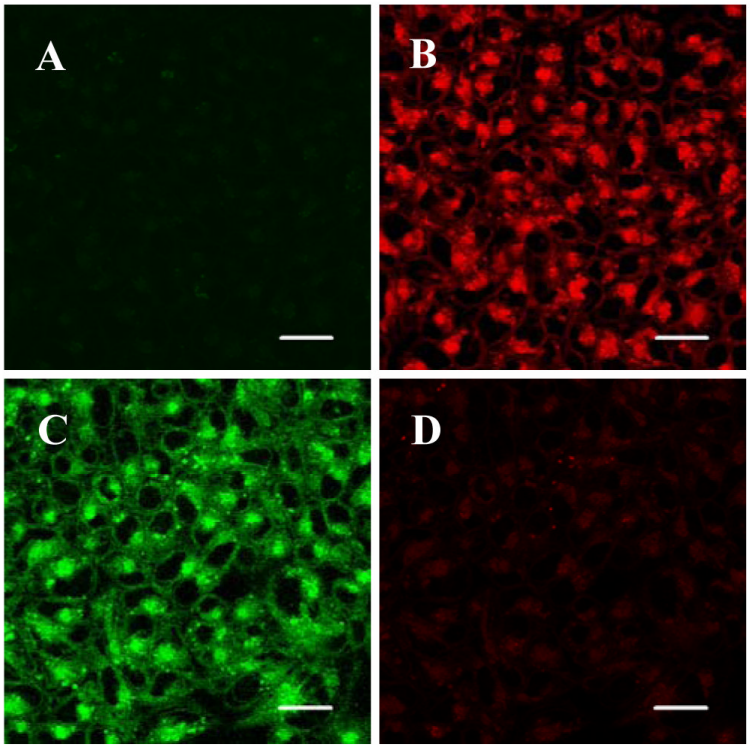

Figure 5.

Initial stage of entry of *cl*-micelles/Cys. In all experiments A2780 cells were transfected with K44A^{dyn}-GFP (dynamin mutant), 16 hr prior to experiments and exposed to DOX-labeled *cl*-micelles/Cys (red) at 37°C for 60 min and analyzed by confocal microscopy. **(A, B)** *cl*-micelles/Cys internalize in cells which are do not express GFP. **(C, D)** Cells transfected with the mutant do not show entry of *cl*-micelles/Cys. **(A, B)** and (**C, D**) are the same cell areas. Cells were exposed to 200 μg/ml of *cl*-micelles/Cys. Bar equals 20 μm.

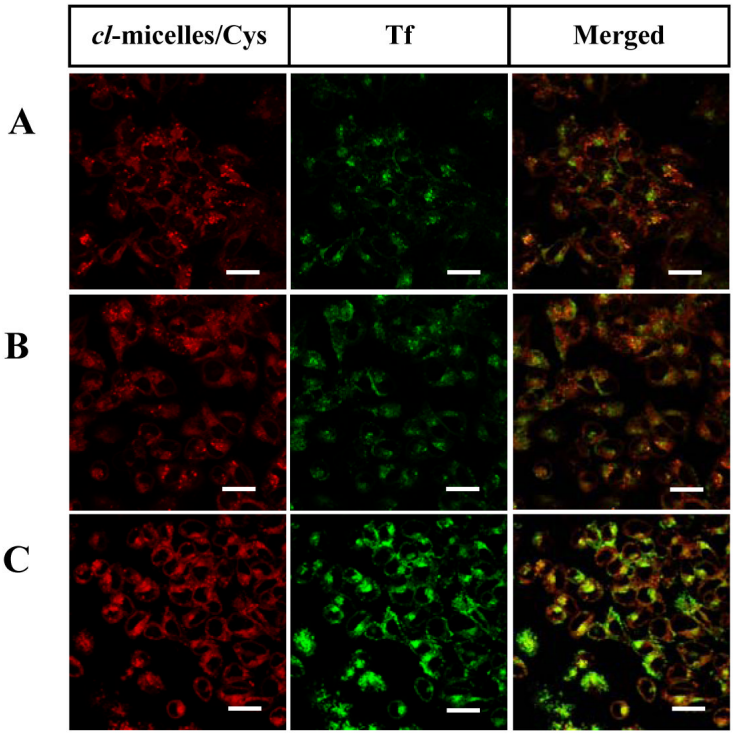

Figure 6.

Cellular uptake of *cl*-micelles/Cys in A2780 cells. A2780 cells were exposed to Dox-labeled *cl*-micelles/Cys for 60 min and then to Alexa 488-labeled Tf (green) for **(A)** 10 min; **(B)** 20 min and **(C)** 30 min at 37°C followed by live cell imaging. In all experiments cells were exposed to 200 μg/ml of *cl*-micelles/Cys. Bar equals 20 μm.

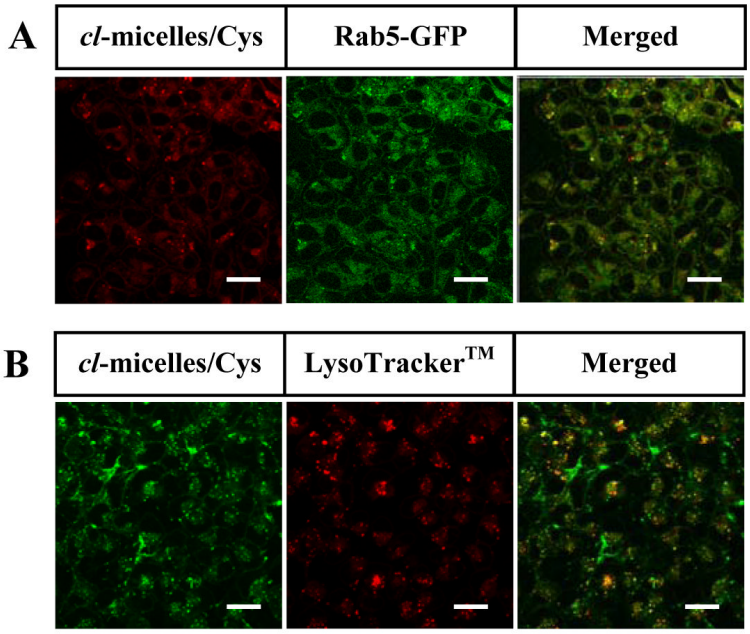

Figure 7.

Intermediate and later stages of entry of *cl*-micelles/Cys. **(A)** A2780 cells transfected with Rab-5 GFP (green) was exposed to DOX-labeled *cl*-micelles/Cys at 37°C for 60 min. **(B)** A2780 were exposed for 60 min. at 37°C to FITC-labeled *cl*-micelles/Cys (Green) and stained with Lysotracker® red (Red) for 10 min. In all experiments, cells were exposed to 200 μg/ml of *cl*-micelles/Cys. Bar equals 20 μm.

Table 1

Physicochemical Characteristics of *cl*-micelles with various types of cross-linker before and after DOX loading at pH 7.0.[a]

	DLS [b]			AFM			TEM	LC [c]
	D_{eff} (nm)	**PDI**	**ζ-potential (mV)**	**Height (H_{ave}, nm)**	**Diameter (D_{ave}, nm)**	**Aspect ratio (D_{ave}/H_{ave})**	**Diameter (nm)**	**(w/w, %)**
cl-micelles/Cys	117.4 ± 5.0	0.06 ± 0.02	−27.8 ± 4.0	5.1 ± 0.2	62.0 ± 0.4	12.2	62.2 ± 3.2	
DOX-loaded *cl*-micelles/Cys	109.9 ± 2.2	0.07 ± 0.01	−14.3 ± 2.5	18.2 ± 2.6	52.9 ± 2.4	2.9	50.6 ± 2.0	51.1 ± 2.0
cl-micelles/ED	214.6 ± 3.1	0.15 ± 0.04	−31.3 ± 3.7	3.0 ± 0.4	114.2 ± 1.6	38.1	83.4 ± 3.5	
DOX-loaded *cl*-micelles/ED	106.2 ± 2.1	0.12 ± 0.04	−14.7 ± 1.3	19.7 ± 2.6	57.4 ± 3.1	2.9	61.4 ± 2.6	50.3 ± 2.1

[a] Targeted degree of cross-linking is 20%.

[b] Effective diameter (D_{eff}), polydispersity index (PDI) and ζ-potential were determined at pH7.0. Notably, the effective diameter of DOX-loaded *cl*-micelles/Cys at pH 7.4 was 111.8 ± 3.5 nm (PDI 0.085 ± 0.02), which was only slightly different from their size at pH 7.0.

[c] Loading capacity (LC) is expressed as mass of incorporated DOX per mass of drug loaded *cl*-micelles (w/w %). DOX-loaded micelles were prepared at R = 0.5 and pH 7.0.

Table 2

Cytotoxic effect of DOX-loaded *cl*-micelles in A2780 ovarian carcinoma cells[a]

Sample	IC_{50} (μg/mL) [b]	Relative Index [c]
DOX	0.024	1
Degradable *cl*-micelles	0.058	2.5
Non-degradable *cl*-micelles	0.381	16.2

[a] The cytotoxicity curves are presented in Supporting information, Figure S7.

[b] IC_{50} (μg/mL) represents the concentration of a drug for 50% inhibition in vitro (n =8).

[c] Relative index represents the IC_{50} ratio between a control and *cl*-micelles for comparison.